Thermal and Structural Characterization of Poly(methylene-1,3-cyclopentane) Samples of Different Microstructures

Odda Ruiz de Ballesteros, Vincenzo Venditto, Finizia Auriemma,* and Gaetano Guerra

Dipartimento di Chimica, Università di Napoli, Via Mezzocannone 4, I-80134 Napoli, Italy

Luigi Resconi

G. Natta Research Center, Himont Italia (A member of the Montedison Group), P. le G. Donegani 12, Casella Postale 155, I-44100 Ferrara, Italy

Robert Waymouth and Anne-Lise Mogstad

Department of Chemistry, Stanford University, Stanford, California 94305

Received July 18, 1994; Revised Manuscript Received November 28, 1994®

ABSTRACT: The thermal properties and the crystalline structure of poly(methylenecyclopentane) samples with different microstructures are investigated. Similar disordered crystalline structures are formed, independently of the microstructure of the sample. These structures present hexagonal packing of the chain axes and extended chains with configurational and conformational disorder, which generate intermolecular rotational and translational disorder. The distance between adjacent parallel chains decreases with the increase of rings with the *cis* configuration; correspondingly, the melting temperature strongly increases. Both interchain distances and melting temperatures seem poorly dependent on the relative stereochemistry between rings. The degree of crystallinity and the correlation length of the crystalline domains tend to increase with the stereoregularity in the configuration of the rings (both *cis* and *trans*). The melting entropy increases with all the examined kinds of stereoregularity (*cis*, *trans*, and isotactic).

Introduction

Cyclopolymerization of 1,5-hexadiene to poly(methylenecyclopentane) was reported by Marvel and coworkers,[1,2] and further investigated by Makowski.[3] Using catalysts derived from $TiCl_4$/Al-*i*-Bu_3 and $TiCl_4$/$AlEt_3$, respectively, both groups reported low activities and incomplete cyclization of the diolefin. More recently, Cheng[4] reported the cyclopolymerization of 1,5-hexadiene using a $TiCl_3/AlEt_2Cl$ catalyst. ^{13}C NMR analysis of the resulting polymer indicated complete cyclization.

For poly(methylene-1,3-cyclopentane), four microstructures of maximum order are possible (Chart 1).[5]

According to the widely accepted cyclopolymerization mechanism proposed by Marvel and Garrison,[1] there are two distinct stereochemical events, for these cyclopolymerizations: olefin insertion and olefin cyclization. The enantioselectivity of the olefin insertion determines the tacticity of the polymer (the relative stereochemistry between the rings), and the diastereoselectivity of the cyclization step determines whether *cis* or *trans* rings are formed.[1,6,7]

Recently, some of us have been investigating group 4 metallocene/methylaluminoxane catalysts for the polymerization of 1,5-hexadiene,[8,9] finding that cyclization is complete also in the case of these homogeneous catalysts. Moreover, depending on the type of cyclopentadienyl ligands in the metallocene complexes, the cyclopolymerization can be, at least partially, diastereoselective. In particular, with achiral zirconocenes, the *cis*/*trans* selectivity can be controlled, leading to the first examples of *trans*-atactic and *cis*-atactic poly-

Chart 1

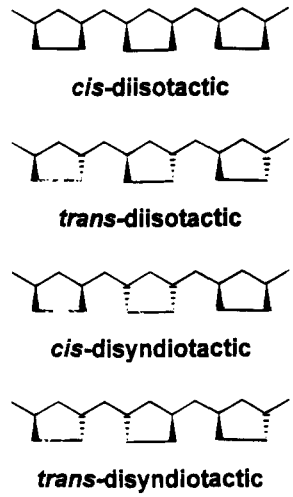

(methylene-1,3-cyclopentane).[8,9] The prevailingly *trans* polymer is obtained in the presence of Cp_2MeX_2 (Cp = cyclopentadienyl; Me = Zr, Hf; X = Cl, CH_3); the prevailingly *cis* polymer is obtained in the presence of the more sterically hindered $Cp^*_2MeX_2$ (Cp^* = pentamethylcyclopentadienyl). This kind of behavior has been rationalized in terms of nonbonded interactions at the model catalytic sites.[6]

Hence, the microstructure of the hexadiene polymers depends on the nature of the catalyst precursor. The microstructures of the polymers obtained with various catalysts are indicated at Table 1. The ratio of *cis* and *trans* rings in the polymer is indicated by the percentage of *cis* rings and were determined by integration of the ^{13}C NMR resonance at 32.2 and 33.5 ppm.[7] The isotacticity of the polymer is reported in terms of α, an

® Abstract published in *Advance ACS Abstracts,* February 1, 1995.

0024-9297/95/2228-2383$09.00/0

Table 1. Microstructural Characterization of PMCP Samples from Different Catalysts[a]

	sample	catalyst	% cis[b]	M_w[c]	α[d]
1	high-*cis*-atactic	$Cp^*_2ZrMe_2$	86	10 000	na[e]
2	random-isotactic	$MgCl_2$/D/$TiCl_4$	52	62 000	0.99[f]
3	*trans*-isotactic	rac-EBI$ZrCl_2$	34	29 200	0.86
4	*trans*-atactic	Ind_2ZrCl_2	37	76 400	0.56
5	high-*trans*-atactic	Cp_2ZrCl_2	19	8 700	0.50

[a] For polymerization conditions, see Experimental Section. [b] Determined from the ratio of ^{13}C NMR resonances at 33.5 and 32.2 ppm. [c] Determined by GPC (1,2,4-trichlorobenzene, 150 °C, vs polystyrene standards). [d] Enantioface copolymerization parameter $\alpha = k_{re}/(k_{re} + k_{si})$. [e] Statistical model not applicable. [f] Sample not completely soluble in 1,1,2,2-tetrachloroethane at 100 °C.

Chart 2

random-isotactic

enantioface copolymerization parameter defined in ref 7 (the enantioface copolymerization parameter, $\alpha = k_{re}/k_{re} + k_{si}$ for k_{re}, k_{si} = rate constants for insertion of the two olefin enantiofaces).

An α-value of 0.5 corresponds to an atactic polymer (samples **4** and **5**) whereas an α-value that approaches 1.0 corresponds to highly isotactic samples (samples **2** and **3**). Analysis of the microstructure of the polymer prepared with $Cp^*_2ZrCl_2$ (sample **1**) reveals an atactic structure with a slight syndiotacticity, which cannot be described in terms of an enantioface copolymerization parameter α.

Using homogeneous metallocene/methylaluminoxane catalysts which exhibit high enantioface selectivities for monomer insertion (in particular, with *rac*-EBI$ZrCl_2$ [EBI = ethylene-1,2-bis(1-indenyl)]), an isotactic polymer (α = 0.86) with 66% *trans* rings has been obtained[7,10] (sample **3**).

The molecular weights of the polymers, determined by GPC vs polystyrene, range from 9000 to 76 000 with the highest molecular weights being obtained with the Ind_2ZrCl_2 and heterogeneous catalyst precursors.

The polymer samples obtained by the heterogeneous Ziegler–Natta catalysts contain *trans* and *cis* cyclopentane rings with a nearly 1:1 ratio and in random sequences. However, due to the high enantioface selectivity of the monomer insertion for these catalyst systems these polymers are highly isotactic, as revealed by ^{13}C NMR. Analysis of the microstructure of polymer **2** prepared with the heterogeneous catalyst reveals a high degree of isotacticity with α = 0.99. This microstructure, called hereafter random-isotactic, is sketched in Chart 2.

Preliminary studies have revealed substantial differences in physical properties (and in particular in the melting temperatures) of samples presenting different *trans*/*cis* ratios for the cyclopentane rings.[9]

The only other structural investigation of these polymers was performed several years ago[3] for a sample obtained from a heterogeneous catalyst. At that time, no information was available from NMR on the microstructure of these polymers. It was suggested, on the basis of the chain identity period (4.8 Å) and of a conformational analysis, that the chains in the crystalline phase consist primarily of units with a *cis* configuration of the cyclopentane rings.

In this paper the thermal properties and the crystalline structure of poly(methylenecyclopentane) samples with different microstructures are investigated. In particular, substantially atactic polymers for which the percent of rings with a *cis* configuration is in the range 86%–19% (samples **1**, **4**, and **5**), as well as two substantially isotactic samples (random-isotactic **2**, and *trans*-isotactic **3**), are considered.

Experimental Section

General Procedures. All polymerizations were carried out under a dry nitrogen atmosphere, using standard Schlenk-tube techniques. Toluene and heptane were purified by refluxing over Al-*i*-Bu_3 and subsequent distillation under nitrogen. Decane was dried over CaH_2. 1,5-Hexadiene (Fluka, 97%) was distilled on a Todd fractional distillation apparatus, collecting the fraction boiling at 59.8–60.2 °C (99.3% pure by GC), which was then vacuum-transferred from CaH_2 and stored under nitrogen. Methylaluminoxane (MAO; Schering 10 w/w % in toluene or Albemarle, 30 w/w % in toluene) was used after removing all volatiles and drying the resulting white powder in vacuo (4 h, 21 °C, 0.1 mmHg). $C_2D_2Cl_4$ (Cambridge Isotopes), Cp_2ZrCl_2 (Boulder Scientific), and $Cp^*_2ZrCl_2$ (Strem) were used as received. $Cp^*_2ZrMe_2$,[11] $B(C_6F_5)_3$,[12] *rac*-ethylenebis(1-indenyl)–$ZrCl_2$ (rac-EBI$ZrCl_2$),[13] Ind_2ZrCl_2,[13] and the heterogeneous, highly isospecific $MgCl_2$/D/$TiCl_4$ (Ti = 3.2%, D = 2,2-diisobutyl-1,3-dimethoxypropane) catalyst[14] were synthesized according to literature preparations.

^{13}C NMR spectra were recorded on a Varian XL-400 (100 MHz) spectrometer. Quantitative ^{13}C NMR spectra were obtained at 100 °C in $C_2D_2Cl_4$ (pulse width 90°; sweep width 60 ppm; delay time >6.5 s or >5 T_1;[15] gated decoupling; peak shifts referenced to the middle of the $C_2D_2Cl_4$ triplet at 74.120 ppm).

Gel permeation chromatography (GPC) analyses were carried out with a Waters 150C high-temperature instrument. The Waters Ultrastyragel columns were eluted with 1,2,4-trichlorobenzene at 150 °C and were calibrated using polystyrene standards.

Synthesis of the Polymers. Sample 1, High-*Cis*-Atactic. $Cp^*_2ZrMe_2$ (7.1×10^{-5} mol) was dissolved in 1,5-hexadiene (33 mL) at room temperature. $B(C_6F_5)_3$ (2.7×10^{-5} mol) was added. The solution turned orange, and a white solid began to precipitate out of solution. The solution was stirred until it became a thick slurry. The resulting polymer was dried in vacuo and obtained as a granular, toluene soluble white powder.

Sample 2, Random-Isotactic. Heptane (360 mL) and 1,5-hexadiene (120 mL) were placed in a 1 L glass reactor at 50 °C. The $MgCl_2$/D/$TiCl_4$ catalyst (73.2 mg, 0.049 mmol of Ti) and Al-*i*-Bu_3 (4.5 mL, Al/Ti 350) were added as a slurry in heptane (5 min aging). The polymerization was continued with stirring for 6 h. After quenching with CH_3OH, the polymer was filtered off, washed with CH_3OH, and dried in vacuo, yielding 64.4 g of spherical, free-flowing particles. The polymer was 30% soluble in xylene at room temperature.

Sample 3, *Trans*-Isotactic. *rac*-EBI$ZrCl_2$ (3.1×10^{-5} mol), MAO (Albemarle; Al/Zr = 1600), decane (6 mL), and toluene (290 mL) were placed in a Schlenk tube at room temperature, and a solution of 1,5-hexadiene (20 mL) and toluene (105 mL) was added dropwise over 3 h. After another 2 h, the reaction was quenched with excess CH_3OH. All volatiles were removed in vacuo. The resulting polymer was dried in vacuo and obtained as toluene soluble, white solid.

Sample 4, *Trans*-Atactic. Ind_2ZrCl_2 (6.42×10^{-5} mol), MAO (Schering; Al/Zr = 1000), toluene (290 mL), and 1,5-hexadiene (120 mL) were placed in a 1 L glass reactor at 20 °C. After 6 h, the reaction was quenched with excess CH_3OH. The resulting polymer was filtered off, washed with CH_3OH, and dried in vacuo, yielding 58 g of a toluene insoluble, white solid.

Sample 5, High-*Trans*-Atactic. Cp_2ZrCl_2 (5.1×10^{-5} mol), MAO (Schering; Al/Zr = 1000), toluene (360 mL), and 1,5-hexadiene (120 mL), were placed in a 1 L glass reactor at −5 °C. After 6 h, the reaction was quenched with excess CH_3OH. The resulting polymer was filtered off, washed with CH_3OH, and dried in vacuo, yielding 18.8 g of a toluene soluble, white powder.

X-ray Diffraction Techniques. X-ray diffraction (XRD) patterns for unoriented samples were obtained by using an automatic Philips powder diffractometer. An approximate evaluation of the degree of crystallinity was obtained by resolving the X-ray diffraction patterns between 2ϑ values of 10 and 25° into a crystalline peak and an amorphous halo and by comparing the areas of the peak and of the halo. Since it was not possible to obtain amorphous samples of PMCP (also by rapid quencing from the melt), the shape of the amorphous halo was taken from the X-ray diffraction patterns of the melt samples. The 2ϑ position of the amorphous halo, at room temperature, was obtained by extrapolation of the X-ray diffraction patterns of at least partially molten samples. As an example, the X-ray diffraction patterns of the *trans*-isotactic sample, recorded at different temperatures in the range 25–110 °C are shown in Figure 1, together with the assumed amorphous halos (dashed lines).

Oriented samples were obtained only for the random-isotactic sample **2** and for the *trans*-isotactic sample **3** by stretching (at room temperature, at a speed of 5 mm/min) strips of compression molded films. Attempts to obtain oriented samples for all the other polymers, also by using different techniques, were unsuccessful, due, in some cases, to the low molecular mass of the samples.

The coherent length of the crystallites in a direction perpendicular to the chain axis (D) was evaluated for the 100 reflection using the Scherrer equation:

$$D = K\lambda/(\beta \cos \vartheta)$$

β being the angular (2ϑ) width of the half-maximum intensity, and taking $K = 0.9$. For $\beta < 1.0°$ (in 2ϑ units), the procedure described in ref 16, for the correction of the half-width for instrumental effects, was applied. In particular, we used a standard quartz specimen having a half-maximum line breadth, under similar geometrical conditions, of 0.18°.

The X-ray diffraction patterns for stretched fibers were obtained by using a Nonius automatic CAD4 diffractometer with Ni-filtered Cu Kα radiation and were collected by always maintaining an equatorial geometry. The measurements have been performed along the reciprocal cylindrical ξ coordinate in the range $0 < \xi < 0.66$ Å^{-1} at intervals of 0.006 Å^{-1} and for $\zeta = l/c$, with $l = 0-4$ and $c = 4.83$ Å, corresponding to the chain identity period.

The Lorentz–polarization (Lp) correction, when used (Figures 3B and 4B), was applied for all the layer lines according to the diffraction geometry ($Lp = (1 + \cos^2 2\vartheta)/\sin 2\vartheta$).

Differential Scanning Calorimetry. A Perkin-Elmer DSC7 was used for the calorimetric analyses. DSC scans were obtained, in a flowing N_2 atmosphere, for heating rates in the range 2.5–20 °C/min.

Dynamic-Mechanical Analysis. The dynamic-mechanical analyses were carried out with a Polymer Laboratories DMTA apparatus at a measurement frequency of 10 Hz and at a heating rate of 4 °C/min. Samples 1 mm thick have been mounted in the bending mode as a single cantilever.

Results and Discussion

X-ray Diffraction of Unoriented Samples. The diffraction profile $I(2\vartheta)$ of the unoriented *trans*-isotactic sample **3** shown in Figure 1A, presents only an intense reflection at $2\vartheta \approx 18°$ and a much weaker reflection at $2\vartheta \approx 32°$.

All the other samples listed in Table 1 present similar diffraction profiles. The Bragg distances of the two reflections for all the samples are listed in Table 2 and indicate the occurrence of a hexagonal packing of the chain axes.

In Figure 2 it is apparent that the distance between adjacent parallel chains in the crystalline phase of PMCP (also indicated in Table 2) decreases with the contents of rings with the *cis* configuration, while it seems poorly dependent on the tacticity (relative stereochemistry between rings).

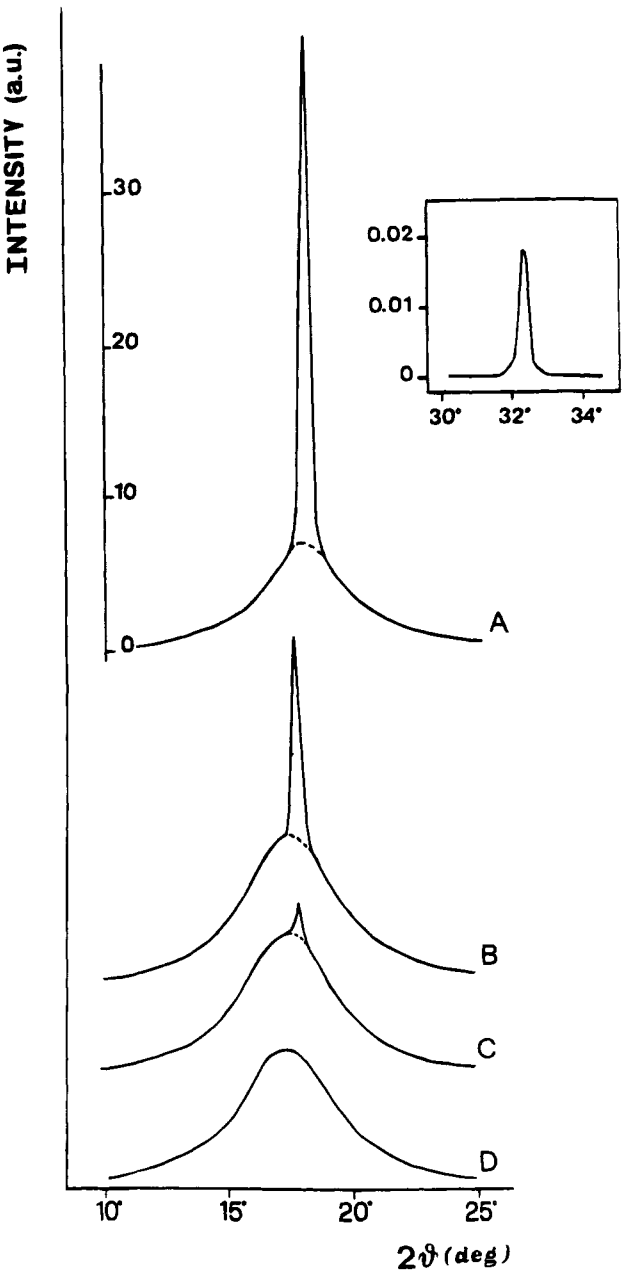

Figure 1. X-ray diffraction powder patterns $I(2\vartheta)$ (au = arbitrary units) of the unoriented *trans*-isotactic sample **3** at different temperatures: (A) 25 °C, (B) 90 °C, (C) 100 °C, (D) 110 °C. For the pattern at 25 °C, the 110 diffraction peak and its relative intensity are also shown (enclosure). Dashed lines show the estimated contribution from the amorphous material.

Table 2. Bragg Distances of the Two Reflections (d_{100} and d_{110}), Interchain Distances (a), Degrees of Crystallinity (x_c), and Coherent Lengths of the Crystallites in the 100 Direction (D)

	sample	d_{100} (Å)	d_{110} (Å)	a (Å)	x_c (%)	D (Å)
1	high-*cis*-atactic	4.80	2.77	5.54	72	700
2	random-isotactic	4.86	2.80	5.61	43	230
3	*trans*-isotactic	4.87	2.81	5.62	39	230
4	*trans*-atactic	4.90	2.82	5.65	48	300
5	high-*trans*-atactic	4.93	2.84	5.69	60	400

Although (as discussed in detail in the next section) there is a large configurational and conformational disorder in the crystalline phase, we still assume for these materials a two-phase (amorphous and crystalline) model. From the diffraction profiles of unoriented samples an approximate evaluation of the degree of

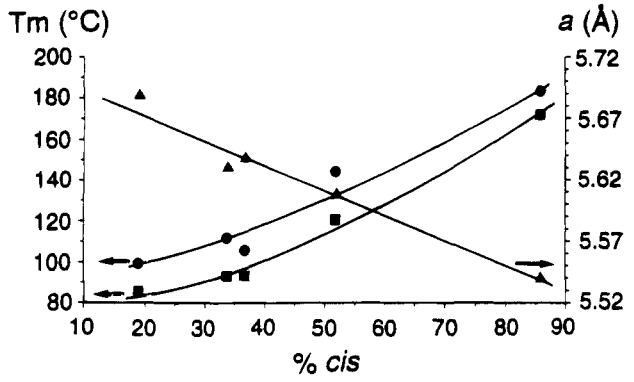

Figure 2. Melting temperatures (left scale, ■ from DSC scans at the heating rate of 10 °C/min, ● equilibrium melting temperature estimates) and interchain distances (right scale, ▲) as a function of *cis* content (%).

crystallinity has been also obtained and has been reported in Table 2.

The coherent length of the crystallites in a direction perpendicular to the chain axis, evaluated on the basis of the half-width of the main equatorial peak, has also been reported in Table 2.

It is apparent that all the samples present a substantial amount of crystallinity, and maximum values of the degree of crystallinity, as well as of the crystal sizes, are obtained for the high-*cis* sample **1** and for the high-*trans* sample **5**.

X-ray Diffraction of Oriented Samples. As described in the Experimental Section, oriented samples were obtained only for the random-isotactic sample **2** and for the *trans*-isotactic sample **3**.

The photographic patterns (not reported here), obtained by a cylindrical camera, show besides the two equatorial reflections (already apparent in the powder spectra of Figure 1) only diffuse streaks along two layer lines. The two layer lines correspond to chain identity periods of 4.83 Å for both samples.

It is reasonable to assume that also the other samples of different microstructures should present similar fiber patterns. The observed small increase of the interchain distance (+1.5%), moving from the high-*cis* sample **1** to the high-*trans* sample **5** (see Table 2) could possibly only correspond (in the hypothesis of similar densities) to a small decrease of the identity period (−3%).

The presence of similar crystalline structures for all the microstructures of PMCP and the high crystallinity of the high-*trans* sample **5** clearly contradict the hypothesis put forth in ref 3 that the crystallizing chains contain primarily *cis* rings.

The XRD intensities, measured by an automatic diffractometer, for an oriented random-isotactic PMCP sample **2** are reported in Figure 3A, for the equator and four layer lines (for the periodicity of 4.83 Å along the chain axes), as a function of the reciprocal lattice coordinate ξ. The diffuse intensity peaks on the layer lines are nearly meridional for $l = 1$, 3, and 4, while the intensity peak for $l = 2$ presents a maximum at $\xi = 0.22$ Å^{-1} with a broad tail reaching also the region with $\xi = 0$). The measured intensities along the meridian (that is for $\xi = 0$) are reported in Figure 4A.

The diffraction intensities, after subtraction of the amorphous halo and correction for the *Lp* factor, are reported for the layer lines in Figure 3B and for the meridian (profile with $\xi = 0$) in Figure 4B.

The patterns of Figure 3 show clearly that the peaks observed in Figure 4 are not true reflections since,

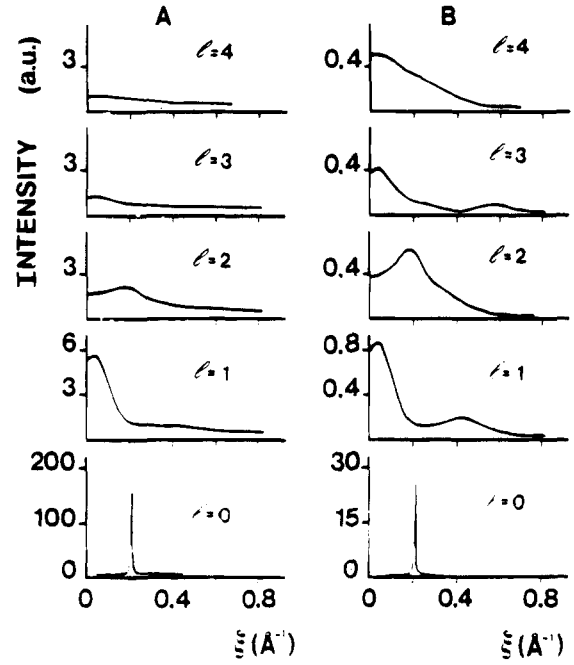

Figure 3. X-ray diffraction intensity (au = arbitrary units) of the oriented random-isotactic PMCP sample **2** vs ξ for the equator and the indicated layer lines l corresponding to a periodicity of $c = 4.83$ Å: (A) experimental, (B) subtracted for the background and corrected by the Lorentz and polarization factor.

although they are sharp along ζ, they are diffuse along ξ. Hence, the indication of a symmetry corresponding to orthorhombic or higher, based on the presence of meridional reflections,[3] has no experimental support.

The presence of only diffuse streaks on the layer lines and of sharp reflections on the equator is typical of a disordered crystalline form in which a long-range positional order for the chain axes is present, while disorder along the chain axes occurs.

In particular, it is reasonable to assume for PMCP a hexagonal packing of the chain axes of extended chains presenting configurational and hence conformational disorder, which generate an intermolecular rotational and translational disorder.

Differential Scanning Calorimetry. The DSC scans of compression-molded PMCP samples on heating and on cooling at a rate of 10 °C/min are shown in Figures 5 and 6, respectively.

The melting and crystallization temperatures (T_m and T_c) and the melting enthalpy (ΔH_m), taken from the scans of Figures 5 and 6, are reported in Table 3.

The enthalpy of melting per gram of crystalline phase ($\Delta H_m'$), calculated on the basis of the degree of crystallinity of Table 2, and the entropy of melting per mol of monomer unit (ΔS_m) are also reported in Table 3.

Of course, the differences in the values of the thermodynamic quantities of Table 3 depend not only on the stereochemistry of the samples but also on the differences in the molecular masses (see Table 1) as well as on possible differences in crystallite size. However, the last contributions to the measured differences are expected to be not substantial.

As far as the molecular masses are concerned, let us recall that macromolecules with at least 1000 atoms do not change significantly in the melting properties on a further increase in molecular size (see ref 17, p 79). For our sample of minimum molecular mass (sample **5**), the

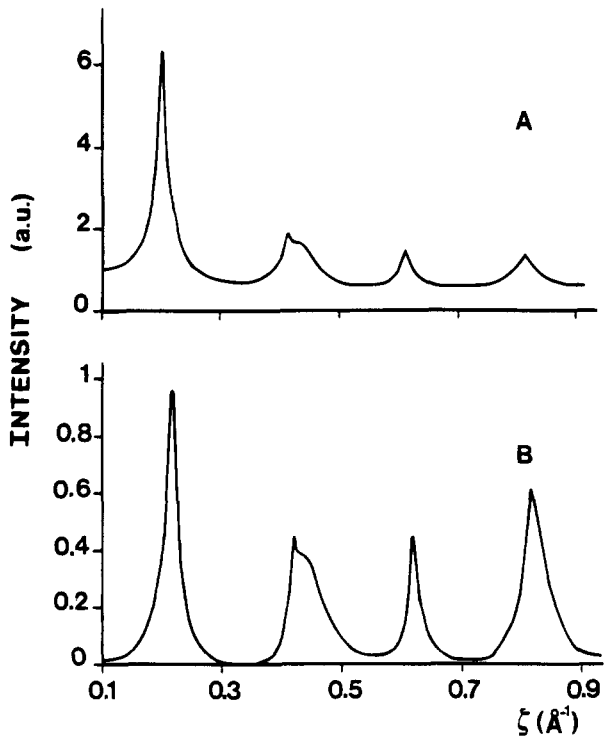

Figure 4. X-ray diffraction intensity (au = arbitrary units) of an oriented random-isotactic PMCP sample on the meridian ($\xi = 0$): (A) experimental, (B) subtracted for the background and corrected by the Lorentz and polarization factor.

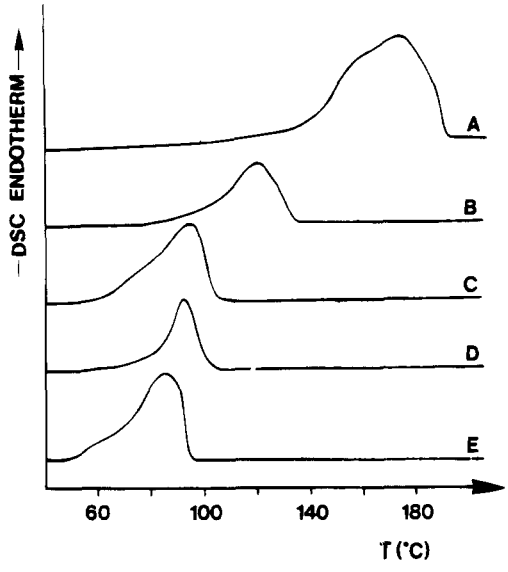

Figure 5. DSC scans, at the heating rate of 10 °C/min, for PMCP samples with different microstructures: (A) high-*cis*-atactic sample **1**, (B) random-isotactic sample **2**, (C) *trans*-isotactic sample **3**, (D) *trans*-atactic sample **4**, (E) high-*trans*-atactic sample **5**.

average number of atoms included in the macromolecules is higher than 1500.

As far as crystallite sizes are concerned, we have, for instance, verified that the differences between the experimental T_m values are close to the differences between possible estimates of the equilibrium thermodynamic values. In particular, the maximum melting temperatures (T_m') obtained by DSC scans, after annealing procedures (of 1 h) at different temperatures (steps of 1 °C), are listed, for all the considered samples, in Table 3.

Table 3. Melting, Equilibrium Melting Estimates, and Crystallization Temperatures (T_m, T_m', and T_c), Melting Enthalpies Referred to the Overall Sample and to the Crystalline Phase (ΔH_m and $\Delta H_m'$), Melting Entropies per Mole of Monomer Unit (ΔS_m), and Glass Transition Temperatures (T_g)

samples	T_m (°C)	T_m' (°C)	T_c (°C)	ΔH_m (J/g)	$\Delta H_m'$ (J/g)	ΔS_m [J/(K mol)]	T_g (°C)
high-*cis*-atactic	171	183	161	59	82	15.0	45
random-isotactic	120	146	94	14	32	6.7	30
trans-isotactic	93	112	44	19	49	11.0	25
trans-atactic	93	106	65	12	24	5.4	30
high-*trans*-atactic	86	100	53	20	33	7.5	25

In Figure 2 it is apparent that the melting temperature (varying from 86 to 171 °C) depends strongly on the *cis* content of the different samples, while, as the interchain distance, it is scarcely dependent on the relative stereochemistry between the rings (e.g. the *trans*-atactic sample **4** and *trans*-isotactic sample **3** present the same T_m value). This suggests that the strong increase of the melting temperature of PMCP with the *cis* content is related to the more efficient lateral packing of the chains, pointed out by the shorter interchain distances (Table 2 and Figure 2).

At variance with the melting temperature behavior, the melting enthalpy per gram of the crystalline phase and the melting entropy tend to increase both with the stereoregularity of the ring conformations and with the tacticity of the polymer. In particular, for the substantially atactic samples (**1**, **4**, and **5**), the highest $\Delta H_m'$ and ΔS_m values are reached by the high-*cis* sample **1**, while increases are also observed going from the *trans* sample **4** to the high-*trans* sample **5**. On the other hand, a comparison of the thermal properties of the *trans*-atactic sample **4** and of the *trans*-isotactic sample **3** (both having a *cis* content close to 35%) shows a dramatic effect, on $\Delta H_m'$ (24 vs 49 J/g) and ΔS_m (5.4 vs 11 J/K mol), of the isotactic stereoregularity between the rings.

It is worth noting that samples **1**, **3**, and **5**, which present the lowest molecular weights (see Table 1), show the highest values of $\Delta H_m'$ (and ΔS_m). Comparison at equal molecular masses should slightly reinforce these differences. In fact, although small effects are expected, the melting enthalpy is usually an increasing function of the molecular weight (ref 17, p 43).

Dynamic-Mechanical Analysis. The storage module E' and loss factor, tan δ, of the compression-molded high-*cis* sample **1** and high-*trans* sample **5** are reported in Figure 7A,B, respectively.

The plots clearly show the glass transition phenomenon which is not seen by DSC measurements.

The temperature corresponding to the maximum of tan δ is taken as the glass transition temperature (T_g) and is reported for all the considered samples in Table 3. It is apparent that there is an increase of T_g with the *cis* content from 25 to 45 °C, but this increase is much smaller than the corresponding increase of the melting temperature.

Conclusions

Similar disordered crystalline structures are formed by PMCP, independently of the microstructure of the sample. These structures present hexagonal packing of the chain axes and extended chains with configurational and conformational disorder, which generate intermolecular rotational and translational disorder.

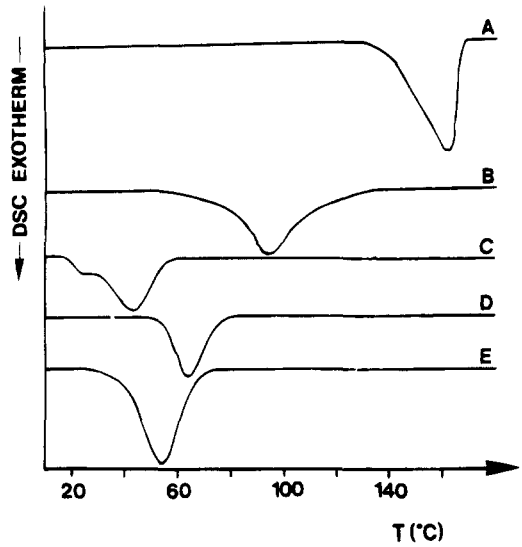

Figure 6. DSC scans, at the cooling rate of 10 °C/min, for PMCP samples with different microstructures: (A) high-*cis*-atactic sample **1**, (B) random-isotactic sample **2**, (C) *trans*-isotactic sample **3**, (D) *trans*-atactic sample **4**, (E) high-*trans*-atactic sample **5**.

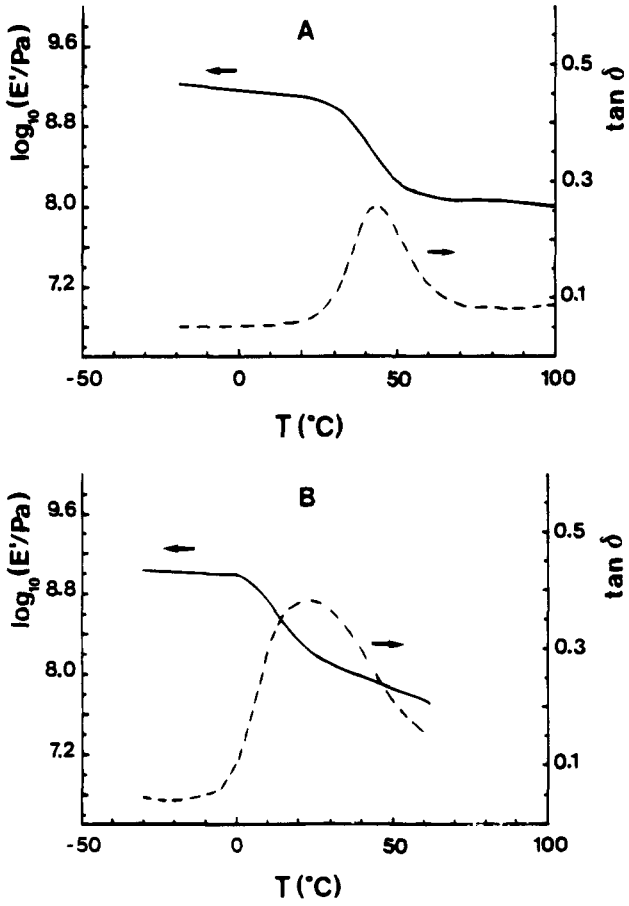

Figure 7. Storage modulus (E', solid line) and loss factor (tan δ, dashed line), from dynamic-mechanical measurements (10 Hz), for two PMCP samples with different microstructures: (A) high-*cis*-atactic sample **1**, (B) high-*trans*-atactic sample **5**.

The distance between the adjacent parallel chains decreases with the content of rings with the *cis* configuration, while it seems poorly dependent on the relative stereochemistry between rings. The degree of crystallinity (which ranges from 39 to 72%), as well as the coherent lengths of the crystalline domains, tends to increase with the stereoregularity in the configuration of the rings (both *cis* and *trans*).

These results contradict a previous hypothesis of crystallizing chains consisting primarily of units with configurationally *cis* rings.[3]

Although the disordered crystalline structures are similar, strong dependences on the microstructure of the melting temperature, enthalpy, and entropy are observed. For instance the melting temperature increases with the *cis* content of the polymers from 86 to 171 °C. This is possibly related to the more efficient packing of the chains, shown by the interchain distances. The entropy of melting increases, instead, with all the examined kinds of stereoregularity (*cis*, *trans*, and isotactic).

By dynamic-mechanical analysis an increase of the glass transition temperature with the content of *cis* rings, from 25 to 45 °C, has also been observed.

A conformational study of PMCP isolated chains with ordered and disordered microstructures is in progress. The aim is to verify the geometrical and energetical feasibility of nearly fully extended chains, independently of the microstructure, and to give more detailed information relative to the chain conformations in the disordered crystalline phase.

A study of the conformational freedom of the isolated chains in the disordered crystalline phase and in the melt, for different microstructures, could also be useful for a possible interpretation of the large variations in the observed melting entropies.

Acknowledgment. This work was supported by the Ministero dell' Università e della Ricerca Scientifica e Tecnologica (Italy). X-ray diffraction data were recorded with a Nonius CAD4 automatic diffractometer (Centro Interdipartimentale di Metodologie Chimico Fisiche, University of Naples). We wish to thank Prof. P. Corradini for the useful discussions, Dr. G. Morini for the preparation of the heterogeneous catalyst, and R. Mazzocchi for preparing the polymer samples.

References and Notes

(1) Marvel, C. S.; Stille, J. K. *J. Am. Chem. Soc.* **1958**, *80*, 1740.
(2) Marvel, C. S.; Garrison, W. E., Jr. *J. Am. Chem. Soc.* **1959**, *81*, 4737.
(3) Makowski, H. S.; Shim, B. K. C.; Wilchinsky, Z. W. *J. Polym. Sci., Part A* **1964**, *2*, 1549.
(4) Cheng, H. N.; Khasat, N. P. *J. Appl. Polym. Sci.* **1988**, *35*, 825.
(5) Farina, M. *Top. Stereochem.* **1987**, *17*, 1.
(6) Cavallo, L.; Guerra, G.; Corradini, P.; Resconi, L.; Waymouth, R. M. *Macromolecules* **1993**, *26*, 260.
(7) Coates, G. W.; Waymouth, R. M. *J. Am. Chem. Soc.* **1993**, *115*, 91.
(8) Resconi, L.; Waymouth, R. M. *J. Am. Chem. Soc.* **1990**, *112*, 4953.
(9) Resconi, L.; Coates, G. W.; Mogstad, A.; Waymouth, R. M. *J. Macromol. Sci.* **1991**, *A28*, 1225.
(10) Coates, G. W.; Waymouth, R. M. *J. Am. Chem. Soc.* **1991**, *113*, 6270.
(11) Manriquez, J.; Mc Alister, D.; Sanner, R.; Bercaw, J. *J. Am. Chem. Soc.* **1978**, *100*, 2723.
(12) Massey, A.; Park, A. *J. Organomet. Chem.* **1964**, *2*, 245.
(13) Lee, I-M.; Gauthier, W.; Ball, J.; Iyengar, B.; Collins, S. *Organometallics* **1992**, *11*, 2115.
(14) Albizzati, E.; Barbè, P.; Noristi, L.; Scordamaglia, R.; Barino, L.; Giannini, U.; Morini, G. *Eur. Pat. Appl.* 361494 A1, **1990**, to Himont.
(15) Schoolery, J. *Prog. Nucl. Magn. Reson. Spectrosc.* **1977**, *11*, 79.
(16) Klug, H. P.; Alexander, L. E. *X-ray diffraction procedure*; John Wiley: New York, 1959; Vol. 9.
(17) Wunderlich, B. *Macromolecular Phisics*; Accademic Press: New York, 1976; Vol. 3.

MA941243C